Glioma-grade diagnosis using in-phase and out-of-phase T1-weighted magnetic resonance imaging: A prospective study

M. de Pardieu, S. Boucebci, G. Herpe, C. Fauche, S. Velasco, P. Ingrand, J.-P. Tasu

Glioma-grade diagnosis using in-phase and out-of-phase T1-weighted magnetic resonance imaging: a prospective study
Short title:

Glioma-grade diagnosis with MRI

Maelys DE PARDIEU [a], Samy BOUCEBCI [a], Guillaume HERPE [a], Cédric FAUCHE [a], téphane VELASCO [a], Pierre INGRAND [b], Jean-Pierre TASU[a, c]

[a] Department of Diagnostic and Interventional Radiology, Poitiers University Hospital, 86000 Poitiers, FRANCE

[b] Epidemiology and Biostatistics, INSERM CIC 1402, Faculty of Medicine and University Hospital, 86000 Poitiers, France

[c] La TIM, INSERM U1101, INSERM-UBO UMR 1101, CHRU Morvan, 29609 Brest, France

*Corresponding author: jean-pierre.tasu@chu-poitiers.fr

Service de Radiologie, CHU de Poitiers, 2 rue de la Milétrie, 86000 Poitiers, France

Abstract

Purpose: The purpose of this prospective study was to determine whether chemical shift gradient echo magnetic resonance imaging (MRI) sequence could predict glioma grade.

Materials and methods: A total of 69 patients with 69 gliomas were prospectively included. There were 41 men and 28 women with a mean age of 50 ± (SD) years (range: 16-82 years). All patients had MRI of the brain including chemical shift gradient echo sequence, further referred to as in- and out-of phase sequence (IP/OP). Intravoxel fat content was estimated by signal loss ratio (SLR= [IP-OP]/2IP)), between in- and out-of-phase images, using a region of interest placed on the viable portion of the gliomas. Association between SLR and glioma grade was searched for using Wilcoxon and Mann-Whitney U tests and diagnostic capabilities using area under the receiver operating characteristics (AUROC) curves.

Results: A significant association was found between SLR value and glioma grade ($P < 0.0001$). SLR > 9 ‰ allowed complete discrimination between grade III and grade II glioma with 100% specificity (95% CI: 85-100%), 100% sensitivity (95% CI: 78-100%) and 100% accuracy (95% CI: 90-100%) (AUROC = 1). A SLR > 20 ‰ allowed discriminating between grade IV and grade III glioma with 75% specificity (95% CI: 57-89%), 73% sensitivity (95% CI: 45-92%) and 72% accuracy (95% CI: 57-84%) (AUC = 0.825, 95% CI 0.702-0.948). The AUROC for the diagnosis of high-grade glioma (grade III and IV *vs.* grade II) was 1.

Conclusion: Chemical shift gradient echo MRI provides accurate grading of gliomas. This simple method should be used as a biomarker to predict glioma grade.

Keywords: Glioma; Chemical shift imaging; Diagnosis; Prospective studies; Biomarkers

List of abbreviations

AUROC: area under the receiving operative curve

CS-GE: chemical shift gradient echo

DWI: diffusion weighted imaging

GE: gradient echo

IP-OP: in- and out-of-phases

MR: magnetic resonance

MRS: magnetic resonance spectroscopy

MRI: Magnetic resonance imaging

ROC: Receiver operating characteristics

ROI: region of interest
SLR: signal loss ratio
T1W: T1-weighted imaging
T2W: T2-weighted imaging
WHO: World Health Organization

Introduction

Glioma refers to any tumors that develops from brain interstitial tissue [1]. The glioma grade is an important issue, as it modifies the management of a glioma and determines the prognosis of the patient. Brain biopsy remains the standard of reference for the grading of gliomas [1]. However, it is an invasive procedure associated with risks of infection and bleeding, in addition to the inherent possibility of sampling error [2]. Magnetic resonance imaging (MRI) is commonly used as the reference imaging method for the follow-up of low-grade and presurgical staging of high-grade gliomas. Enhancement of glioma after intravenous administration of a gadolinium chelate indicates blood–barrier breakdown and/or neovascularity, which is a typical feature of high-grade glioma [3]. However, glioma grading using contrast enhancement is sometimes unreliable due to a high rate of false-positive findings [4]. Several studies have tested the capabilities of MRI for glioma grading [5-11] and others have validated the relationship between the metabolites detected by MR spectroscopy (MRS) and glioma grading [12-15]. However, MRS has several drawbacks. Multi-voxel MRS requires a long acquisition time and is sensitive to magnetic susceptibility artifacts due to adjacent bones, internal foci of hemorrhage, motion artifacts and/or poor shimming [16].

The chemical shift in- and opposed-phase (IP-OP) sequence is a gradient-echo (GE) MRI sequence, currently utilized to detect lipids in several organs [17-20] . A recent study has shown its usefulness in the detection of lipids, including in gliomas [21]. In high-grade gliomas, elevated lipid levels display a greater signal loss on opposed-phase images [21]. Ramli et al. demonstrated that lipids causing signal loss on IP-OP sequence were similar to visible lipids and that the degree of signal drop strongly correlated with glioma grade [17]. The results of this study that included only 22 patients with four of them with grade III gliomas were further confirmed later by the same group with a larger retrospective study including 40 patients [22]. To date, no prospective study has assessed the capabilities of IP-OP MRI in predicting glioma grade in a large cohort of patients.

The purpose of this study was to prospectively determine whether chemical shift gradient echo MRI could predict glioma grade.

Materials and methods

Patients

A prospective study was conducted in a single center from April 2016 and June 2017. Inclusion criteria included: (*i*), patient age > 18 years; (*ii*), preoperative MRI examination was needed; and (*iii*), surgery for glioma was performed less than one month after MRI examination. Exclusion criteria were: (*i*), poor quality MRI examination; (*ii*), MRI protocol deviation without chemical shift imaging; and (*iii*), previous treatment for glioma before MRI. Ethical approval was obtained from the local institutional review board committee (N°00317). All patients provided written informed consent.

MRI protocols

All patients underwent a standard brain MRI protocol with three different MRI equipments, including T1-weighted, T2-weighted, diffusion-weighted imaging (DWI) and T1-weighted images obtained after intravenous administration of a gadoterate meglumine (Dotarem®, Guerbet) at the dose of 0.2 mL/Kg, at a flow rate of 2 mL/second. Additionally, in and out-of-phase imaging was performed before intravenous administration of contrast material in the axial plane adapted according to the equipment used as follows:

(*i*), Magnetom® Aera 1.5 Tesla (Siemens Healthiners); 64 sections were obtained in 41 sec using the following parameters: 5-mm slice thickness, 10° flip angle, 280 mm field of view, a 256 × 256 matrix size, TR=8.05 msec, TE_{out} = 2.38 msec and TE_{in} = 4.76 msec.

(*ii*), Skyra® 3 Tesla (Siemens Healthiners)**;** 96 sections were obtained in 68 sec with the following parameters: 3-mm slice thickness, 9° flip angle; 285-mm field of view; 320 × 320 matrix size, TR = 8 msec, TE_{in} = 2.46 msec and TE_{out} = 3.69 msec.

(*iii*), Magnetom® Verio 3 Tesla (Siemens Healthiners)**;** 96 sections were obtained in 68 sec using the following parameters: 3-mm slice thickness, 9° flip angle, 285 × 285 field of view, 320 × 320 matrix size, TR = 8 msec, TE_{in} = 2.46 msec and TE_{out} = 3.69 msec.

Image analysis

A neuroradiologist with 10 years of experience (S.B.) and one resident with 2 years of experience in neuroradiology (M.P.) performed in consensus all measurements on a dedicated neuro-imaging station (OleaSphere® software, Version 2,2, 2016; Olea Medical). The portion of the glioma displaying isosignal on T1-weighted images and iso to hyperintense signal on T2W images was considered as a solid portion regardless of the presence or absence of glioma enhancement. The portion of the glioma exhibiting a hypointense signal on T1W images and hyperintense signal on T2W images was considered as the necrotic or cystic portion. Considering the internal heterogeneity of the glioma, five regions of interest (ROIs) were placed on the solid portion in the in-phase images. ROIs on the opposed-phase images were then automatically placed from the position of the ROI on the in-phase image (Figure 1). ROI areas were kept to around 5.0 mm^3 in size.

Signal loss ratio (SLR) was then computed according to the following equation:

$$SLR = \frac{IP - OP}{2 \times \text{IP}}$$

where IP represents the mean ROI signal value obtained from IP sequence and OP represents the mean ROI signal value obtained from OP sequence.

Standard of reference

Histopathological analyses were performed according to the World Health Organization (WHO) guidelines [1]. According to the WHO-2007 classification diffuse gliomas were graded as WHO grade II (low grade), WHO grade III (anaplastic) or WHO grade IV (glioblastoma). Nuclear atypia, mitotic activity, necrosis, and florid microvascular proliferation were used for the grading of diffuse gliomas,. Diffuse astrocytic neoplasm without marked mitotic activity, necrosis or florid microvascular proliferation (MVP) was diagnosed as low-grade diffuse astrocytoma, irrespective of the degree of nuclear atypia. Anaplastic astrocytoma corresponded to glioma with marked mitotic activity. The presence of necrosis and/or florid MVP leads to the diagnosis of glioblastoma. According to pathological diagnosis, three groups of patients were considered for the statistical analysis, grade II, III and IV. Low grade gliomas including Grade II whereas Grade III and Grade IV were considered as high grades.

Statistical analysis

Statistical analysis was performed on SAS software (version 9.4, SAS institute, Cary, NC, USA). Quantitative variables were expressed as means standard deviation [SD] and range, or medians and ranges, and qualitative variables as raw numbers, proportions and percentages. Wilcoxon and Mann-Whitney tests were used to search association between SLR and glioma grades. The capabilities of IP-OP MRI for the diagnosis of were evaluated in terms of sensitivity, specificity and accuracy with their corresponding 95% CIs. The discriminatory capability of SLR for glioma grade obtained with IP-OP MRI was evaluated using a receiving operative curve (ROC) analysis with a calculation of area under the curve (AUC). A subgroup analysis was performed to search for differences according to MRI equipment. To assess a potential machine effect in the relation between SLR and glioma grade, a two-factor analysis of variance (ANOVA) with interaction was performed. Statistical significance was set at $P < 0.05$.

Results

Seventy-nine patients were initially included. Ten patients were secondarily excluded, 3 for poor quality MR images and 7 for protocol deviation. Figure 2 gives the flow chart of the study.

The final study population included 69 patients (28 women and 41 men) with a mean age of 50 ± 17 (SD) years (range: 16- 82-years). The median time between MRI examination and histopathological confirmation was 15 days (range: 1 – 115 days). Sixty-seven (67/69; 97%) patients underwent surgical excision allowing complete histopathological analysis of gliomas. The remaining two patients underwent stereotaxic biopsies leading to a final diagnosis of Grade IV glioma for each. Histopathologically, 22/69 gliomas (32%) were Grade II, 15/69 (22%) Grade III and 32/69 (46%) Grade IV. No tumors were infra-tentorial in location.

Table 1 presents the characteristics of patients and the main results. A significant difference in SLR was observed between glioma grades ($P < 0.0001$) (Fig.3). A cut-off value of 20 ‰ for SLR yielded 75% sensitivity (24/32; 95% CI: 45-92%), 73% specificity (11/15; 95% CI: 57-89%) and 72% accuracy (34/47; 95% CI: 57-84%) for the diagnosis of Grade III glioma vs. Grade IV glioma, with an AUROC of 0.825 (95% CI: 0.702 - 0.948) (Fig. 4). A cut-off value of 9‰ for SLR (or any value between 8.82 and 9.75 ‰) allowed differentiating Grade III glioma from Grade II glioma with 100% sensitivity(15/15; 95% CI: 78 - 100%),

100% specificity of 100% (22/22; 95% CI 85 - 100%) an 100% accuracy(37/37; 95% CI: 90 - 100%), with an AUROC of 1 corresponding to a perfect separation for the two grades (Figure 5). The AUROC for the diagnosis of high-grade gliomas (grade III and IV *vs.* grade II) was 1.

Two-factor ANOVA confirmed a significant difference of mean SLR between grades ($P < 0.0001$) and revealed no interaction between machine and grade ($P = 0.40$) and no significant machine effect ($P = 0.30$).

Discussion

Our results suggest that SLR values obtained from chemical shift MRI can help discriminate between glioma grades (II, III and IV). By comparison with MRS, IP-OP MRI can detect intratumoral fat content with a shorter acquisition time, a wide availability on all MRI devices, and no requirement for specific expertise.

In our study, we found a partial overlap in SLR between Grades III and IV gliomas. However, this result has not substantial inconvenience in clinical practice because gliomas with these two grades require the same therapeutic management. In addition, It should be noted that grade IV gliomas, unlike grade III ones, usually exhibit typical characteristics such as internal necrosis, heterogeneous contrast enhancement and rapid growth [23].

Our results are in line with those of two previous studies [17, 21]. Lim et al. showed that lipid content was more frequently associated with malignant brain lesions than with benign ones in a group of patients with benign, malignant and infectious intra axial brain lesions [21]. However, in this study it is not clear if histopathological confirmation was obtained from all lesions. Ramli et al. specifically studied a group of patients with gliomas [17]. These authors suggested that SLR can serve as a parameter for discriminating between the different glioma grades. However, the limited number of patients, particularly those with Grade III gliomas (only 4 among 22 gliomas) and the pathological confirmation obtained from biopsies which could introduce sample bias, were limitations of this study. Indeed, the pathology analysis from tissue samples is an imperfect gold standard because of sampling error with regard to the possible heterogeneity of gliomas.

Seow et al. proposed glioma lipid quantification using lipid distribution mapping based on IP-OP images [22]. They showed that mean SLR of the solid region of the glioma is useful for discriminating between glioma grades but with an overlap for Grade II and Grade III gliomas. However, in this study, as in the previous ones, SLR was computed from the formulae IP-OP/IP [17, 21, 22]. In our study, we used a different formula (*i.e.*, IP-OP/2IP) for

fat quantification. This formula is in fact the correct one; SLR, or fat signal fraction is computed from the formula F/(W+F) where W and F are the signal contributions from water and fat. For IP-OP imaging, even though the water and fat signals are not separated, a fat signal fraction can be calculated from IP = W+F and OP = W-F. Consequently, SLR= F/(W+F) = [(W+F) - (W-F)] / 2 (W+F) = IP-OP/2IP. The discrepancies in terms of cut-off proposed by previous studies can therefore be explained by this difference.

Fat content from SLR could be based on three different MRI acquisition methods, 2, 3 or 6 time points (respectively dual-echo, OP and IP, dual-dual-echo or six echos). Each method demonstrates some degrees of measurement error, but the six-echo method seems to have the highest degree of accuracy. Indeed, this model accounts for the signal loss due to magnetic field inhomogeneity (T2* decay), not corrected in case of dual echo, which can lead to an underestimation of fat content at a maximum of around 30% particularly for low-fat content [24]. Otherwise, a T1 effect can also introduce an overestimation in the range of 1.5-3.5% [25]. Despite these potential biases and approximations, satisfactory accuracy was demonstrated by the use of dual echo in clinical practice [24]. In addition, this method is the widely used technique and the results obtained in our study demonstrate that this method can be clinically effective.

Both conventional and advanced MRI sequences, such as MRS, DWI, perfusion imaging, diffusion kurtosis imaging, and radiomics have been widely evaluated so as to develop a non-invasive method for the glioma grading. While all of them seem useful, they may remain complex to implement or not available everywhere. Further studies are nevertheless required to compare these methods.

Our study has several limitations. First, we did not evaluate MRS or MR fat saturation methods, or other methods of fat spectral modeling. However, accuracy of the fat content measurement obtained by the in-out-phase sequence was not part of the study design and was assessed in a previous study [17]. Second, reproducibility measure of SLR was not studied but a previous report on the liver demonstrated strong reproducibility with an intraclass correlation coefficient at 0.85 [24]. Third, glioma heterogeneity could introduce bias in SLR measurement. We choose to measure SLR of the solid glioma portion since it is the best area for glioma grading [17, 22]. In addition, considering the heterogeneity of the glioma, 5 measurements were performed to obtain a mean SLR value to limit the impact of potential tumor heterogeneities. Nevertheless, further studies are required to evaluate reproducibility of SLR measurement in gliomas. Finally, the use of 3 different MRI devices with 2 different magnetic fields might have, in theory, introduced bias. However, it was shown that the impact

of magnet field strength is negligible compared to the values of SLR [26]. The method might therefore be applicable at both 1.5- and 3-T.

In conclusion, chemical shift gradient echo MRI provides accurate grading of gliomas. A discriminating cut-off value of 9 ‰ for SLR, allows predicting high-grade gliomas with 100% sensitivity and 100%specificity. This simple method should be used in routine as a biomarker to predict glioma grade.

Disclosure of interest

The authors declare that they have no competing interest in relation with this article.

Credit author statement

All authors certify that they have participated sufficiently in the work including participation in the concept, design, analysis, writing, or revision of the manuscript in the same degree.

Authorship contribution statement

All authors attest that they meet the current International Committee of Medical Journal Editors (ICMJE) criteria for Authorship.

Acknowledgements

The authors would like to thank M Jeffrey Arsham for his useful contribution in English reviewing of this manuscript.

References

[1] Izquierdo C, Joubert B, Ducray F. Anaplastic gliomas in adults: an update. Curr Opin Oncol 2017;29:434-442.

[2] Brandner S, Jaunmuktane Z. Neurological update: gliomas and other primary brain tumours in adults. J Neurol 2018;265:717-727.

[3] Chow D, Chang P, Weinberg BD, Bota DA, Grinband J, Filippi CG. Imaging genetic heterogeneity in glioblastoma and other glial tumors: review of current methods and future directions. AJR Am J Roentgenol 2018;210:30-38.

[4] Peng X, Yishuang C, Kaizhou Z, Xiao L, Ma C. Conventional magnetic resonance features for predicting 1p19q codeletion status of World Health Organization grade II and III diffuse gliomas. J Comput Assist Tomogr 2019;43:269-276.

[5] Yang Y, Yan LF, Zhang X, Nan HY, Hu YC, Han Y, et al. Optimizing texture retrieving model for multimodal MR image-based support vector machine for classifying glioma. J Magn Reson Imaging 2019;49:1263-1274.

[6] Wei J, Yang G, Hao X, Gu D, Tan Y, Wang X, et al. A multi-sequence and habitat-based MRI radiomics signature for preoperative prediction of MGMT promoter methylation in astrocytomas with prognostic implication. Eur Radiol 2019;29:877-888.

[7] Vamvakas A, Williams SC, Theodorou K, Kapsalaki E, Fountas K, Kappas C, et al. Imaging biomarker analysis of advanced multiparametric MRI for glioma grading. Phys Med 2019;60:188-198.

[8] Li X, Liao S, Hua J, Guo L, Wang D, Xiao X, et al. Association of glioma grading with inflow-based vascular-space-occupancy MRI: a preliminary study at 3T. J Magn Reson Imaging 2019;

[9] Juratli TA, Tummala SS, Riedl A, Daubner D, Hennig S, Penson T, et al. Radiographic assessment of contrast enhancement and T2/FLAIR mismatch sign in lower grade gliomas: correlation with molecular groups. J Neurooncol 2019;141:327-335.

[10] Wang B, Zhao P, Zhang Y, Ge M, Lan C, Li C, et al. Quantitative dynamic susceptibility contrast perfusion-weighted imaging-guided customized gamma knife re-irradiation of recurrent high-grade gliomas. J Neurooncol 2018;139:185-193.

[11] Yamashita K, Hatae R, Hiwatashi A, Togao O, Kikuchi K, Momosaka D, et al. Predicting TERT promoter mutation using MR images in patients with wild-type IDH1 glioblastoma. Diagn Interv Imaging 2019;100:411-419.

[12] Gao W, Wang X, Li F, Shi W, Li H, Zeng Q. Cho/Cr ratio at MR spectroscopy as a biomarker for cellular proliferation activity and prognosis in glioma: correlation with the expression of minichromosome maintenance protein 2. Acta Radiol 2019;60:106-12.

[13] Andronesi OC, Arrillaga-Romany IC, Ly KI, Bogner W, Ratai EM, Reitz K, et al. Pharmacodynamics of mutant-IDH1 inhibitors in glioma patients probed by in vivo 3D MRS imaging of 2-hydroxyglutarate. Nat Commun 2018;9:1474.

[14] Ditter P, Hattingen E. Magnetic resonance spectroscopy of brain tumors. Radiologe 2017;57:450-458.

[15] Suh CH, Kim HS, Jung SC, Choi CG, Kim SJ. 2-Hydroxyglutarate MR spectroscopy for prediction of isocitrate dehydrogenase mutant glioma: a systemic review and meta-analysis using individual patient data. Neuro Oncol 2018;20:1573-1583.

[16] Callovini GM. Is it appropriate to redefine the indication for stereotactic brain biopsy in the MRI Era? Correlation with final histological diagnosis in supratentorial gliomas. Minim Invasive Neurosurg 2008;51:109-113.

[17] Ramli N, Khairy AM, Seow P, Tan LK, Wong JH, Ganesan D, et al. Novel application of chemical shift gradient echo in- and opposed-phase sequences in 3 T MRI for the detection of H-MRS visible lipids and grading of glioma. Eur Radiol 2016;26:2019-2029.

[18] Crombé A, Alberti N, Catena V, Buy X, Kind M. Spontaneous rupture of a retroperitoneal lymphangioma: understanding chylous signal with chemical-shift and TrueFISP MR sequence. Diagn Interv Imaging 2018;99:761-763.

[19] Kirchgesner T, Perlepe V, Michoux N, Larbi A, Vande Berg B. Fat suppression at three-dimensional T1-weighted MR imaging of the hands: Dixon method versus CHESS technique. Diagn Interv Imaging 2018;99:23-28.

[20] Schieda N, Lim RS, McInnes MDF, Thomassin I, Renard-Penna R, Tavolaro S, Cornelis FH. Characterization of small (<4cm) solid renal masses by computed tomography and magnetic resonance imaging: current evidence and further development. Diagn Interv Imaging 2018;99:443-455.

[21] Lim CJ, Ng KH, ramli N, Azman RR. Evaluation of the application of chemical shift for the detection of lipid in brain lesion. Radiography 2011;17:43-48.

[22] Seow P, Narayanan V, Hernowo AT, Wong JHD, Ramli N. Quantification and visualization of lipid landscape in glioma using in -and opposed-phase imaging. Neuroimage Clin 2018;20:531-6.

[23] Fayed N, Davila J, Medrano J, Olmos S. Malignancy assessment of brain tumours with magnetic resonance spectroscopy and dynamic susceptibility contrast MRI. Eur J Radiol 2008;67:427-433.

[24] Mashhood A, Railkar R, Yokoo T, Levin Y, Clark L, Fox-Bosetti S, et al. Reproducibility of hepatic fat fraction measurement by magnetic resonance imaging. J Magn Reson Imaging 2013;37:1359-1370.

[25] Yu H, Shimakawa A, Hines CD, McKenzie CA, Hamilton G, Sirlin CB, et al. Combination of complex-based and magnitude-based multiecho water-fat separation for accurate quantification of fat-fraction. Magn Reson Med 2011;66:199-206.

[26] Kim HJ, Cho HJ, Kim B, You MW, Lee JH, Huh J, et al. Accuracy and precision of proton density fat fraction measurement across field strengths and scan intervals: a phantom and human study. J Magn Reson Imaging 2018.

Figure Captions

Figure 1. 67 year-old man with grade IV glioma. A region of interest was placed on in-phase gradient echo (A) and on out-of-phase image (B). A region of interest (arrows) was placed on the viable part of the glioma to calculate the mean signal on each image. Signal loss ratio was then calculated.

Figure 2. Study flow chart.

Figure 3. Graph shows box plots of signal loss ratio (SLR) according to glioma grade. Vertical lines through each box represent SLR ranges. Boxes stretch across interquartile range (i.e., from lower quartile to upper quartile). The horizontal lines inside the boxes represent the median values.

Figure 4. Graph shows sensitivity as a function of 1 minus specificity for the diagnosis of Grade IV glioma against Grade III glioma using signal loss ratio (SLR). AUROC = area under the receiving operative curve.

Figure 5. Graph shows sensitivity as a function of 1 minus specificity for the diagnosis of Grade III glioma against Grade II glioma using signal loss ratio (SLR).

Table 1. Demographics data and signal loss ratio results according to glioma grade in 69 patients.

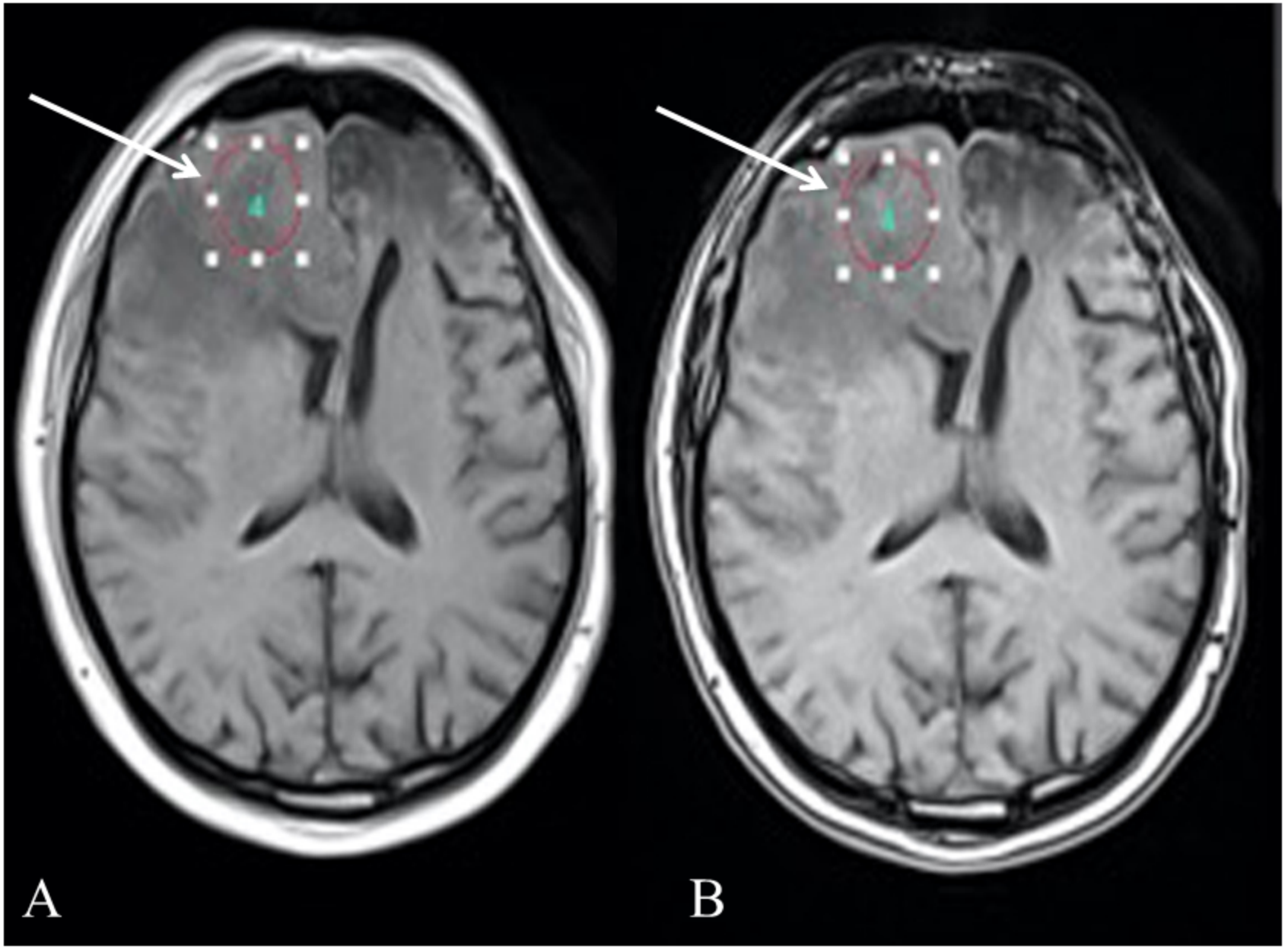
A
B

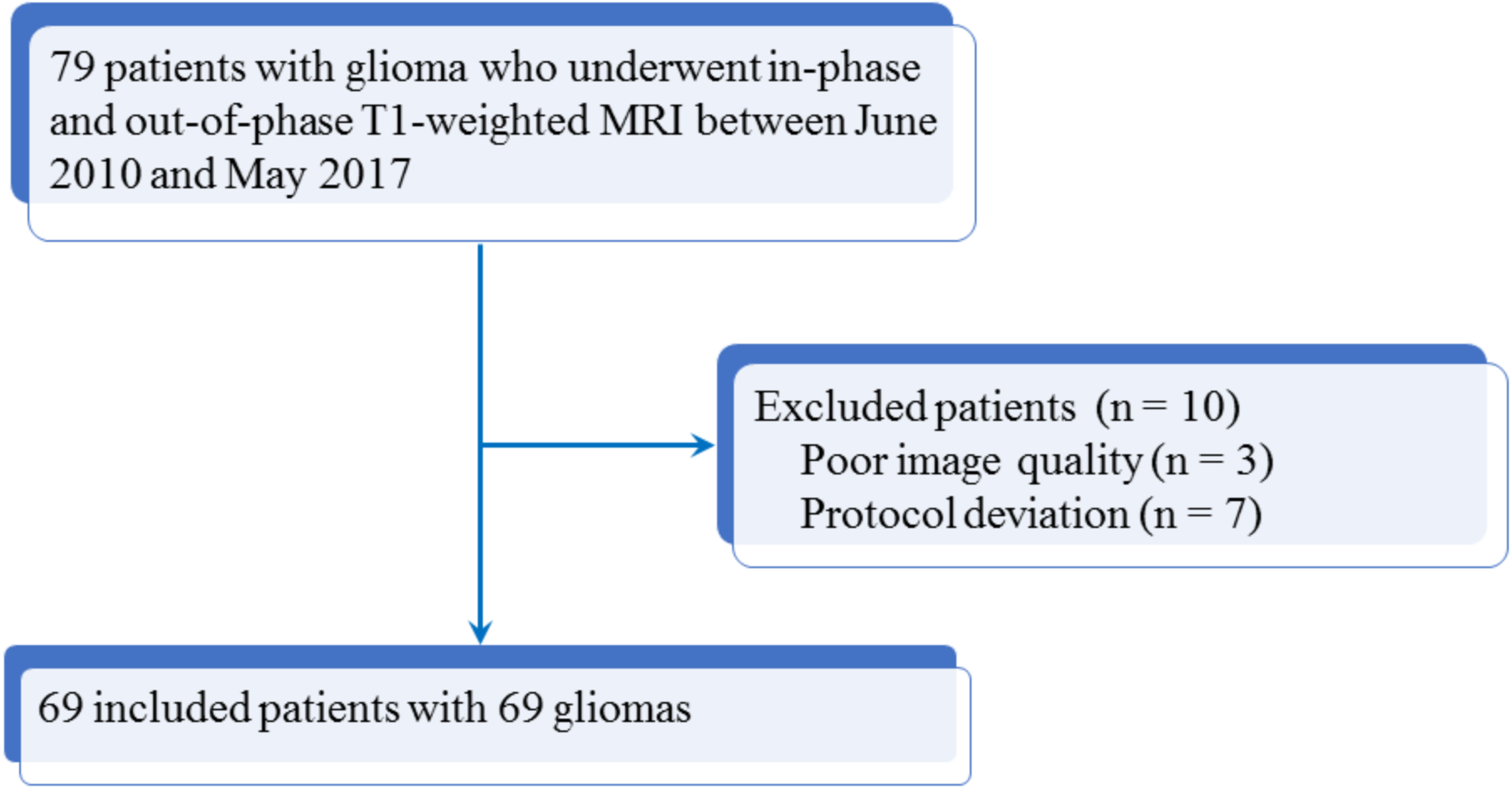
79 patients with glioma who underwent in-phase and out-of-phase T1-weighted MRI between June 2010 and May 2017
Excluded patients (n = 10)
Poor image quality (n = 3)
Protocol deviation (n = 7)
69 included patients with 69 gliomas

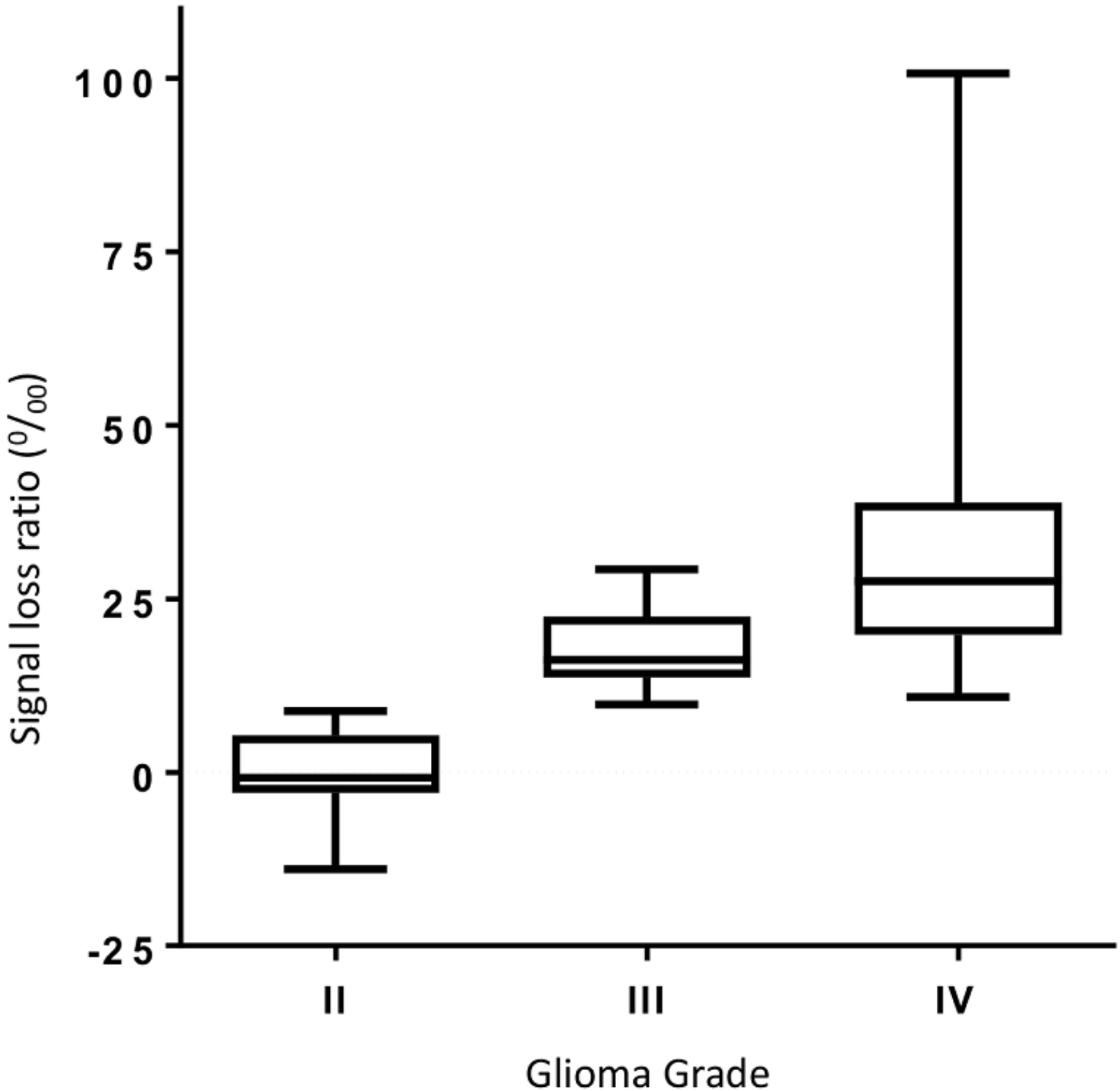
100
75
50
25
0
-25
Signal loss ratio (‰)
II
III
IV
Glioma Grade

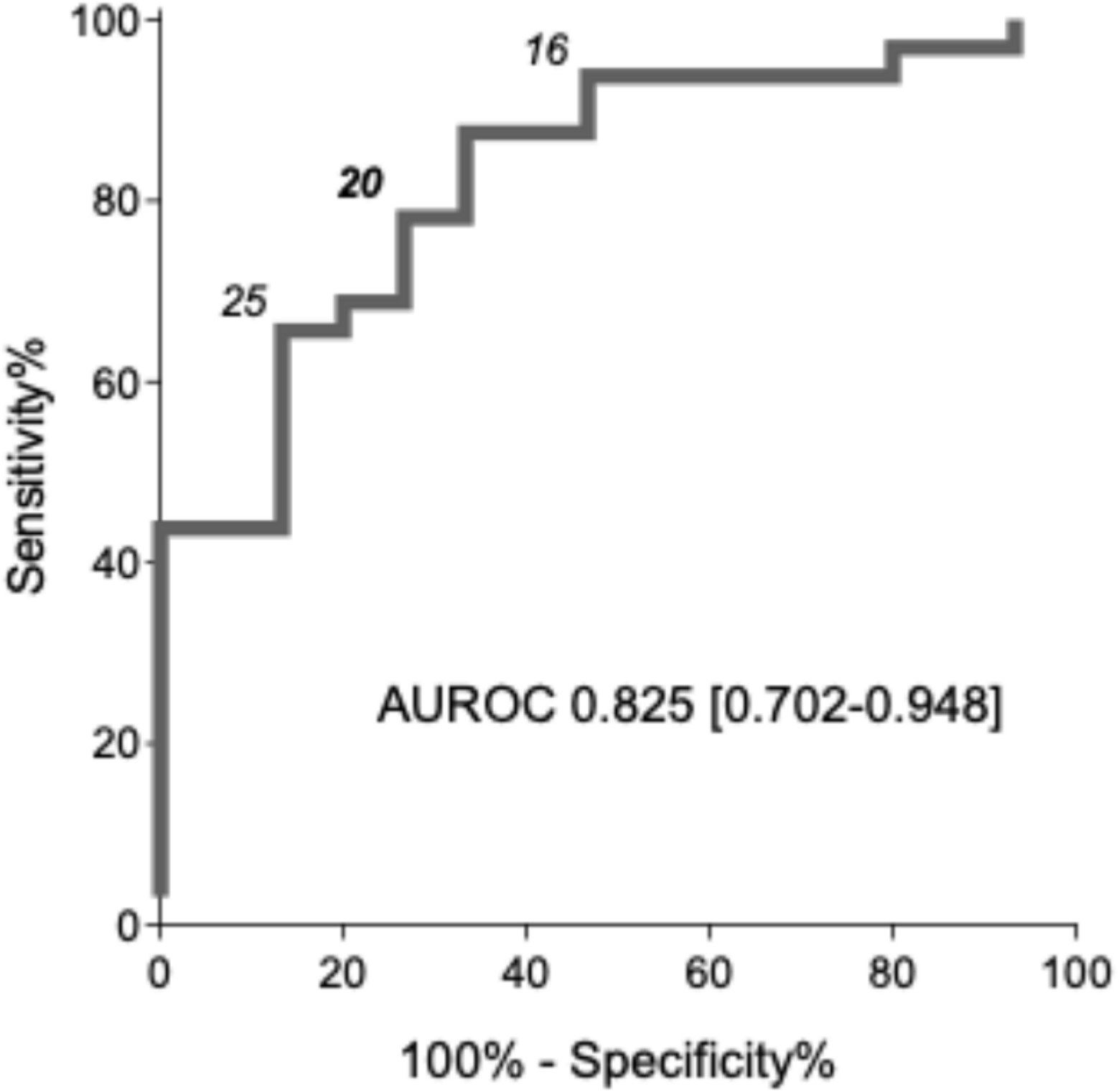
100
80
60
40
20
0
Sensitivity%
16
20
25
AUROC 0.825 [0.702-0.948]
0
20
40
60
80
100
100% - Specificity%

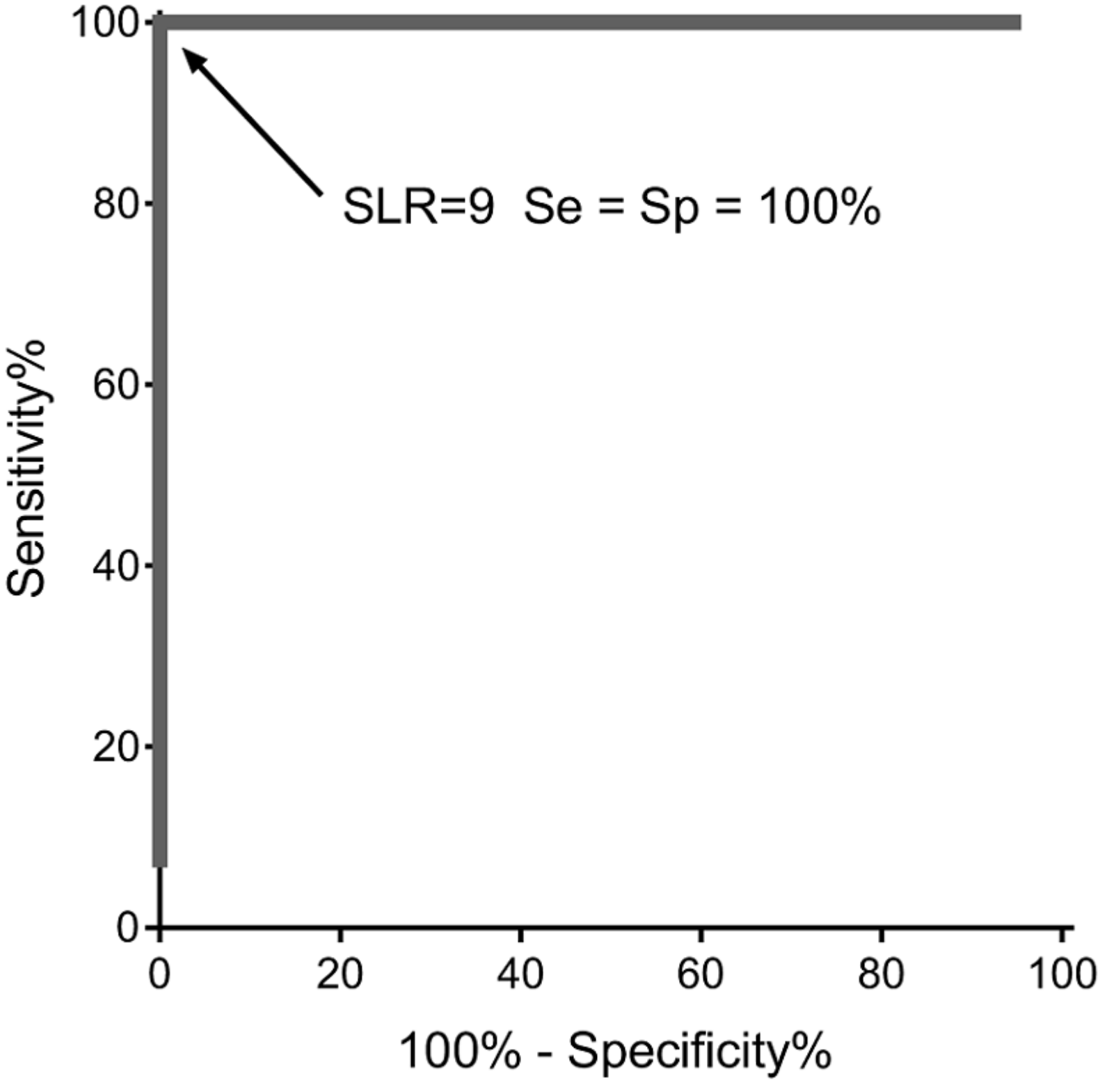
100
80
60
40
20
0
Sensitivity%
SLR=9 Se = Sp = 100%
0
20
40
60
80
100
100% - Specificity%

	Grade II (n = 22)	Grade III (n = 15)	Grade IV (n = 32)
Male Female	13 (13/22; 59%) 9 (9/22; 41%)	9 (9/15; 60%) 6 (6/15; 40%)	19 (19/32; 59%) 13 (13/32; 41%)
Age (years)	39 ± 14 [17 - 66]	48 ± 17 [19 - 76]	59 ± 16 [6 - 82]
Mutation	Oligodendroglioma IDH mutation (n= 3) Astrocytoma IDH WT (n=19)	Anaplasic oligodendroglioma, IDH mutation; 1p19q co-deletion; R132H + (n =3) Anaplasic astrocytoma IDH WT (n = 6) Anaplasic astrocytoma IDH mutation (n = 6)	IDH mutation (n = 5) IDH WT (n = 27)
Mean SLR (°/₀₀)	-0.06 ± 6.18 [-13.94 - 8.82]	17.92 ± 5.91 [9.75 - 29.25]	32.31 ± 18.06 [29.25 - 100.71]
Median SLR (Q1; Q3) (°/₀₀)	-0.78 (-2.91; 5.32)	16.20 (13.68; 22.43)	27.53 (19.82; 37.94)

With; IDH= isocytrate dehydrogenase; WT= wild type; SLR= signal loss ratio, Q = quartile
Quantitative variables are expressed as mean ± standard deviations; numbers in brackets are ranges. Qualitative variables are expressed as raw numbers; numbers in parentheses are proportions followed by percentages.